Journal of Atmospheric and Solar-Terrestrial Physics 73 (2011) 534–543

Contents lists available at ScienceDirect

Journal of Atmospheric and Solar-Terrestrial Physics

journal homepage: www.elsevier.com/locate/jastp

Decrease of Schumann resonance frequencies and changes in the effective lightning areas toward the solar cycle minimum of 2008–2009

A. Ondrášková *, S. Ševčík, P. Kostecký

Department of Astronomy, Physics of the Earth and Meteorology, Faculty of Mathematics, Physics and Informatics, Comenius University, 84248 Bratislava, Slovakia

ARTICLE INFO

Article history:
Received 5 February 2010
Received in revised form
4 November 2010
Accepted 8 November 2010
Available online 20 November 2010

Keywords:
Schumann resonances
11-year solar cycle
Thunderstorm
Ionosphere

ABSTRACT

For the period 1988–2002, it has been shown that the SR mode frequencies and Q-factors decrease with the decrease of X-ray radiation toward the solar cycle minimum (Sátori et al., 2005). In the present study, a decrease of frequencies and Q-factors of all first four SR modes from the latest solar cycle maximum to the anomalous minimum of 2008–2009 is found using the data from Modra Observatory. Decreases obtained here for the first two SR modes are evidently greater than those obtained in the study cited above. Moreover, effective thunderstorm areas are calculated from the monthly mean diurnal frequency range of the electric field component. Our study reveals that the difference between the northern and the southern hemisphere summer areas not only declines with the decrease in solar activity but almost vanishes during the deep solar minimum of 2008–2009. Semi-annual variation in the areas dominates in years of the deep solar minimum.

1. Introduction

The cavity between the conductive Earth and the conductive ionosphere is a global spherical waveguide for electromagnetic waves, which are permanently excited by the lightning activity predominantly in the three major regions: Maritime Continent, Africa and South America. Schumann (1952) predicted theoretically the existence of the resonant modes, called Schumann resonances (SR), due to interference of the electromagnetic waves within the Earth-ionosphere waveguide. These resonance modes are in the extremely low frequency (ELF) range and they are close to 8, 14, 20, 26 Hz, etc.

The diurnal and seasonal variability of the SR parameters (peak frequency, relative amplitude and quality factor) for individual modes have been studied by, e.g. Balser and Wagner (1960), Ogawa et al. (1969), Nickolaenko and Rabinowicz (1995), Sátori and Zieger (1996), Sátori (1996), Price and Melnikov (2004) and Ondrášková et al. (2007).

Several studies have documented that SR parameters vary on the 11-year time scale of the solar cycle (Sátori et al., 2000, 2005; Füllekrug et al., 2002; Kulak et al., 2003). A decrease of all modal frequencies and Q-factors from the solar cycle maximum to the minimum in 1996–1997 was found. For example, a decrease of the yearly mean of the first mode frequency by 0.07 Hz was found at Nagycenk from the electric field component, by 0.13 Hz at Arrival Heights in the Antarctic and by 0.2 Hz at Rhode Island (USA) from the magnetic field component (Sátori et al., 2005). Using a two-characteristic layer model of the lower ionosphere (Greifinger et al., 2007) these changes in SR frequencies can be interpreted as the X-ray induced modification of the conductivity profile confined to the upper characteristic layer (Sátori et al., 2005). The sensitivity of the upper characteristic layer's position on the X-ray flux variation is logarithmic, hence the hundredfold decrease of the X-ray flux over the solar cycle causes only a small change in conductivity profile and thus a relatively small change in the SR frequencies (Sátori et al., 2005).

The diurnal frequency range (DFR) of SR is the band in which the resonance frequency shifts up and down during the day. This variation of frequency is caused by daily movement of the continental-size lightning region (source of the SR) from one continent to another around the globe, i.e. source–observer distance (SOD) changes for a fixed observational site. The value of DFR is related to the size of this lightning region, which is in theoretical considerations approximated by a single circular area moving along the equator. The wider the region, the smaller the DFR, and vice versa (Nickolaenko and Rabinowicz, 1995; Nickolaenko and Hayakawa, 2002) and this is valid for each SR mode. This relation for the first two SR modes is demonstrated in Sátori et al. (2009, Figure 16.8) where DFRs and satellite observations of the three main lightning region diameters are compared. All three main lightning areas are greater in Northern Hemisphere (NH) summer than in Southern Hemisphere (SH) summer due to the greater land areas there. Moreover, having a record of daily variations of the SR mode frequency derived from the vertical electric field component one can evaluate the effective source width using the "calibrating curve" (Nickolaenko and Rabinowicz, 1995; Nickolaenko and

* Corresponding author. Tel.: +421 2 60295469; fax: +421 2 65425982.
E-mail address: adriena.ondraskova@fmph.uniba.sk (A. Ondrášková).

1364-6826/$ - see front matter © 2010 Elsevier Ltd. All rights reserved.
doi:10.1016/j.jastp.2010.11.013

Hayakawa, 2002). It can be assumed that an increase/decrease of the effective lightning area means an increase/decrease of real thunderstorm areas.

Nickolaenko and Rabinowicz (1995) found a nonlinear relation between the effective lightning area and the lightning flash rate, showing that the former can be considered a measure of the latter. Indeed, Sátori and Zieger (2003) studied the areal variations of the global lightning activity on different timescales and showed that the annual and semi-annual areal variations exhibit decadal (11-year) modulations.

Furthermore, it was shown that the intensity of SR is linked to the temperature of the tropical atmosphere (Williams, 1992). The link is a lightning flash rate, which increases nonlinearly with temperature. Thus, the yearly mean of the effective lightning area can be considered a measure of the mean temperature.

According to NASA web page (http://www.nasa.gov/topics/solarsystem/features/solar_minimum09.html) the present solar cycle minimum of 2008–2009 was extraordinarily deep. There were no sunspots observed on 266 of the year's 366 days (73%) in 2008. Sunspot counts for 2009 dropped even lower. As of March 31st, there were no sunspots on 78 of those 90 days (87%). That was the quietest sun we have seen in almost a century. Careful measurements by several NASA spacecraft showed that the sun's brightness dropped by 0.02% at visible wavelengths and 6% at extreme UV wavelengths since the solar minimum of 1996. The X-ray radiation, which ionizes the Earth's atmosphere and is responsible for the conductivity profile of the ionosphere, was by an order of magnitude lower than in solar cycle minima studied previously (http://goes.ngdc.noaa.gov/data/avg/).

In this paper, we present results of measurements of the electric field SR component from October 2001 to July 2009 at the Modra Observatory. This nearly 8-year interval is long enough to resolve the SR parameter variability on the 11-year time scale using the data from the solar cycle maximum to the anomalous solar cycle minimum in 2008–2009. More pronounced variations are expected in this minimum, which differs from the minimum studied by Sátori et al. (2005). Areas of the effective global lightning regions are calculated from our SR data and variations of these areas from the solar cycle maximum toward this deep minimum are analysed too.

2. Measuring equipment and data processing

Monitoring of the vertical electric field SR component has been performed at the Astronomical and Geophysical Observatory (AGO) of Comenius University near Modra, Slovakia (48.37 N, 17.27 E, 530 m a.s.l.). From October 2001 to July 2009 there were practically no interruptions except for the six cases when measuring hardware or software was being updated or repaired, which lasted about a month, or short interruptions due to power outages or unfavourable weather situations (in some cases days).

The electric field SR component is recorded with a capacitive (ball) antenna mounted on a 5 m insulator mast. Details are given in Kostecký et al. (2000) and in Ondrášková et al. (2007).

Since October 2001 through July 2006, the raw time series data were collected every half hour for 327.68 s (which is 65,536 samples taken with 200 Hz sampling frequency), supplying 48 files per day. In the following text, this regime is referred to as a Measurement Regime 1 (MR1). Since then data of the same length have been collected more frequently: every 6 min, i.e. 240 files are stored per day. This regime is referred here as a Measurement Regime 2 (MR2).

Each sequence of data was subjected to discrete Fourier transform (DFT). The frequency resolution of the obtained spectrum is 3.05 mHz. These raw SR spectra from Modra observatory (AGO) up to August 4, 2009, can be viewed at a new address at http://195.80.191.82/.

In the second step, the raw spectra were smoothed with 25-point moving averages. To remove the low-frequency noise the frequency range 6–45 Hz was retained from DFT spectra for further processing. Then the principal parameters for the first five modes (frequency F, quality factor Q and amplitude A) were computed by the least square method (LSM) fitting of spectra by the sum of five Lorentz functions. Subroutines from the GSL library (http://www.gnu.org/software/gsl) were implemented in the fitting code. The fitting process was performed in a modified way as given in Ondrášková et al. (2007). Since therein the dispersion of output parameters (e.g. frequency) was too great in some months, the whole investigated period was once more processed with more strict criteria for selection of "good" results of the fitting process and, moreover, for five modes. The following ranges of frequencies and Q-factors were applied: mode 1 (7.2–8.2 Hz; 1.2–10), mode 2 (13.0–15.0 Hz; 1.4–10), mode 3 (19.2–21.4 Hz; 2–11), mode 4 (24.8–27.5 Hz; 2–12) and mode 5 (31–33 Hz; 2–12). This modification of criteria removed majority of bad results of the fitting process while the patterns of the diurnal variations of SR modes remain essentially the same as in Ondrášková et al. (2007).

There are other techniques for determining the modal frequencies. Sátori et al. (2009) used a method of the complex demodulation. It has been shown that slightly different values for frequency can be produced with different methods. This may affect the DFR evaluation and subsequently the absolute values of the effective lightning areas.

In order to find the influence of the last solar cycle on the SR the satellite data of X-ray fluxes were used. Geostationary Operational Environmental Satellites (GOES) have an unobstructed view of the sun for all but the few dozen hours per year when the Earth eclipses the sun. Ion chamber detectors provide whole-sun X-ray fluxes for the 0.05–0.3 nm (0.05–0.4 nm prior to GOES-8) and 0.1–0.8 nm wavelength bands. We used 5 min averages of the GOES-10 0.1–0.8 nm data as they are available in the whole studied period. These data, available through the Solar-Terrestrial Physics Division of the National Geophysical Data Centre, were used to calculate daily and monthly averages.

3. Diurnal frequency variations

Generally, the diurnal frequency variation pattern of each mode is predominantly determined by the source–observer geometry (Sátori et al., 2003; Sátori et al., 2009). The variations in frequency for the electric field component for the first, second and third SR modes obtained here are shown in Figs. 1–3, respectively. There are graphs of the diurnal variation of frequency for every month of the year and for about 8 years of measurements. These plots were obtained from monthly means of peak frequencies using Bézier spline interpolation (GNUPLOT package), which seems to be more suitable for the determination of representative daily variation for a given month than "classical" cubic splines. Moreover, still slightly scattered values of frequencies from the Lorentzian fitting process called for some kind of interpolation.

The overall pattern in the whole year corresponds to the annual transition from the "winter-type" to the "summer-type" diurnal frequency variation and back to the "winter-type" one. Latitudinal movement of the sources over the year can explain the observed annual changes in the pattern of the diurnal variation.

Generally, thanks to the proximity of the two observatories, our diurnal frequency variation curves are very similar to the curves obtained at Nagycenk in 1993–1995 (Sátori and Zieger, 1996). On the other hand, a slight difference can be seen if our results are compared with the diurnal frequency variation of the first 3 modes

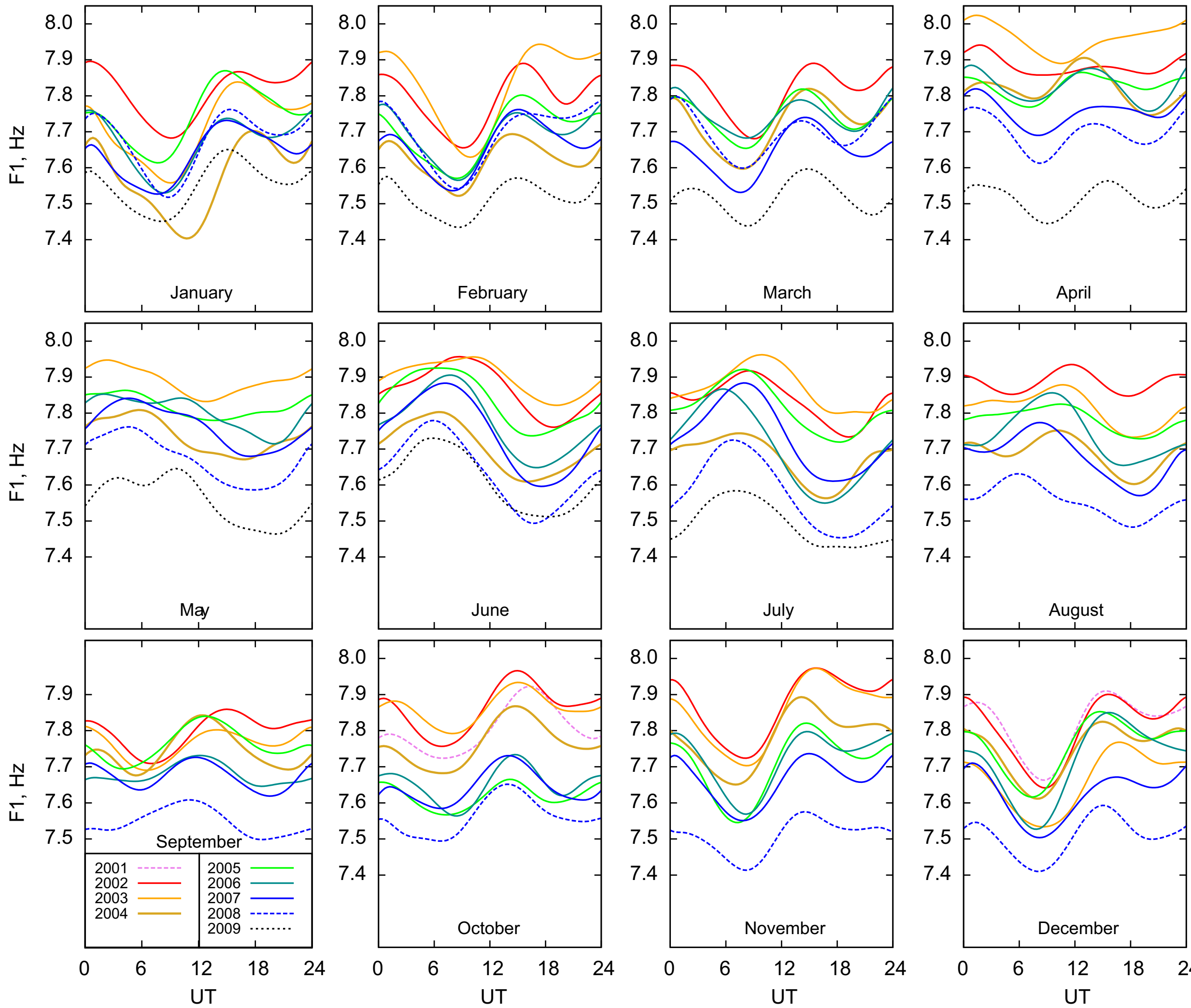

Fig. 1. Monthly averaged diurnal variations of the first mode frequency in the years 2001–2009. In black and white version the different bold lines are used for years of the solar cycle maximum, and different thin lines for years of the solar cycle minimum. Colour appears in web version. Note the analogical patterns in different years in all months. October 2001 through July 2006 data are taken every half hour (measurement regime MR1). Fine details on the diurnal pattern since August 2006 are caused by the use of "6-minute" data (measurement regime MR2).

reported by Price and Melnikov (2004, last column in Fig. 4 therein), which is given as a 3-month average variation calculated from 4-year averages. This difference arises from the different SOD of the Mitzpe Ramon station in Israel. Secondly, comparison with the Price and Melnikov curves of the diurnal variation is not completely appropriate due to the fact that they show 3-month averages.

As expected from the theory our average diurnal frequency patterns are different for the three modes and each mode shows a distinct seasonal variation. This has been already reported by Sátori and Zieger (1996). The curves for the first mode show only one primary maximum and one minimum in frequency, with their times varying with the season. In winter months (November–March) the minimum frequency occurs at Modra at about 9 UT, while in June–July the first mode frequency has its minimum in afternoon hours and maximum around 9 UT.

Sátori and Zieger (1996) have shown that the transition from the winter to the summer pattern occurs in some years in April and in other years in May. As can be seen from Fig. 1, curves for May have indications of the summer pattern in 2004–2009. In June and July, all curves exhibit the summer pattern, which persists in August 2006, 2007 and 2008. Thus our study reveals a tendency that the summer-type diurnal variation shortens during the studied solar cycle maximum and lengthens during the studied minimum. Nevertheless, the summer-type diurnal variation lasts shorter than the winter-type diurnal variation in all phases of the studied solar cycle.

The pattern of the diurnal variation for higher modes is an increasingly humped curve as the number of nodal lines grows with growing mode number, which follows from the form of zonal harmonics (Legendre polynomials) (Nickolaenko, 1997). The diurnal variation of the second mode as observed at Modra is depicted in Fig. 2. The MR1 data were used in the period October 2001–July 2006. The MR2 data are available since August 2006 and the corresponding curves show more pronounced humps than in previous years. In winter, the curves reveal a deep minimum at around 14 UT and two maxima at 2 and 20 UT. A secondary minimum is more pronounced in 2007–2009, i.e. in years when MR2 data collection was used. As this pattern repeats in the mentioned 3 years and in all winter months, it must be a real feature. April and September are transition months when the winter pattern of the diurnal variation changes for the summer one and vice versa. In summer months there is a wide maximum around 12 UT in years of the solar cycle maximum, which splits into two maxima in 2007–2009, when MR2 data are available.

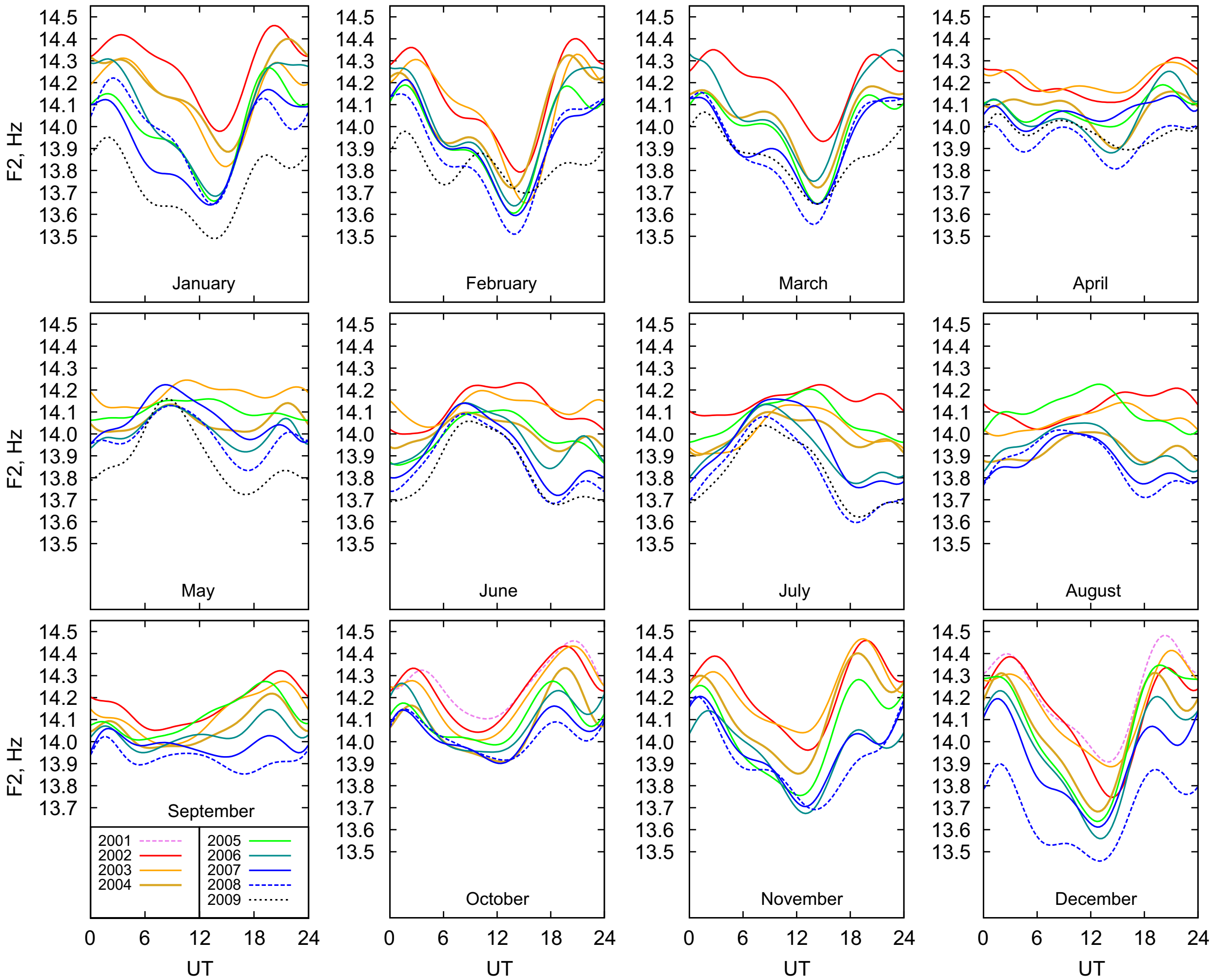

Fig. 2. The same as in Fig. 1 but for the second mode frequency.

The diurnal frequency variation of the 3rd mode is depicted in Fig. 3. Similar to the second mode, the fine details are more pronounced since August 2006 when MR2 data are used.

Fig. 4 shows a combination of diurnal and annual frequency variations from January 2002 to July 2009 as pseudo-three-dimensional maps. Maps for modes one through four are arranged from left to right; the data for years 2002 through 2009 from top to bottom. The white points or areas represent the missing, unreliable or out-of-range data. The diurnal frequency variations from Figs. 1–3 seem to be visible also in maps in Fig. 4. Unfortunately, the "map form" cannot show them in detail.

On the other hand, considering the inter-annual variations, a comparison between subsequent years 2002–2009 shows that the frequencies monotonically decrease. This clear decrease of the mean diurnal frequency level, which appears in all modes with the same sign, can be attributed to changes in conductivity of ionospheric layer toward the solar cycle minimum (Sátori et al., 2005) and to a diminished wave speed within the Earth-ionosphere cavity. Details of this decrease are discussed in Section 5.

4. The diurnal frequency range and the effective source width

In order to obtain a consistent homogeneous database, all our data were selected in all years in the MR1 (i.e. with the measurement duration of 327.68 s each half hour) and this selection was used for the computation of the DFR values, i.e. the difference between the maximal and the minimal frequencies on a diurnal curve.

The first and the second mode DFRs are listed in Tables 1 and 2, respectively, and depicted in upper graph in Fig. 5. In a month when we do not have a DFR value due to measurement interruption the DFR value is calculated as an average of the value in the same month a year before and a year after that month.

Comparing with DFR values from Nagycenk we find systematically higher values of our DFRs. This difference can be attributed to our method for determining the peak SR frequencies using Lorentzians and subsequent fitting the diurnal variation by Bezier splines while Nagycenk frequencies were determined by the complex demodulation method. Therefore, the absolute values of the source widths, calculated below, will be smaller but the trends or periodical changes are not dependent on the technique of DFR determination.

Theoretical calibration curves, which allow us to transform the $DFR = F^{MAX}(t) - F^{MIN}(t)$ in Hz into the effective source width measured in hours, depend primarily on the position of observational site. Calibration curves were computed for a model based on the assumption that the lightning discharges were uniformly distributed in a single circular area and its diameter is measured in hours. The centre of this area moved uniformly along the equator. The propagation constants at resonant frequencies were derived from experimental data (Bliokh et al., 1980) and their values in the whole SR frequency range was calculated by interpolation and extrapolation. The calibration curves computed for Nagycenk (47.6°N,

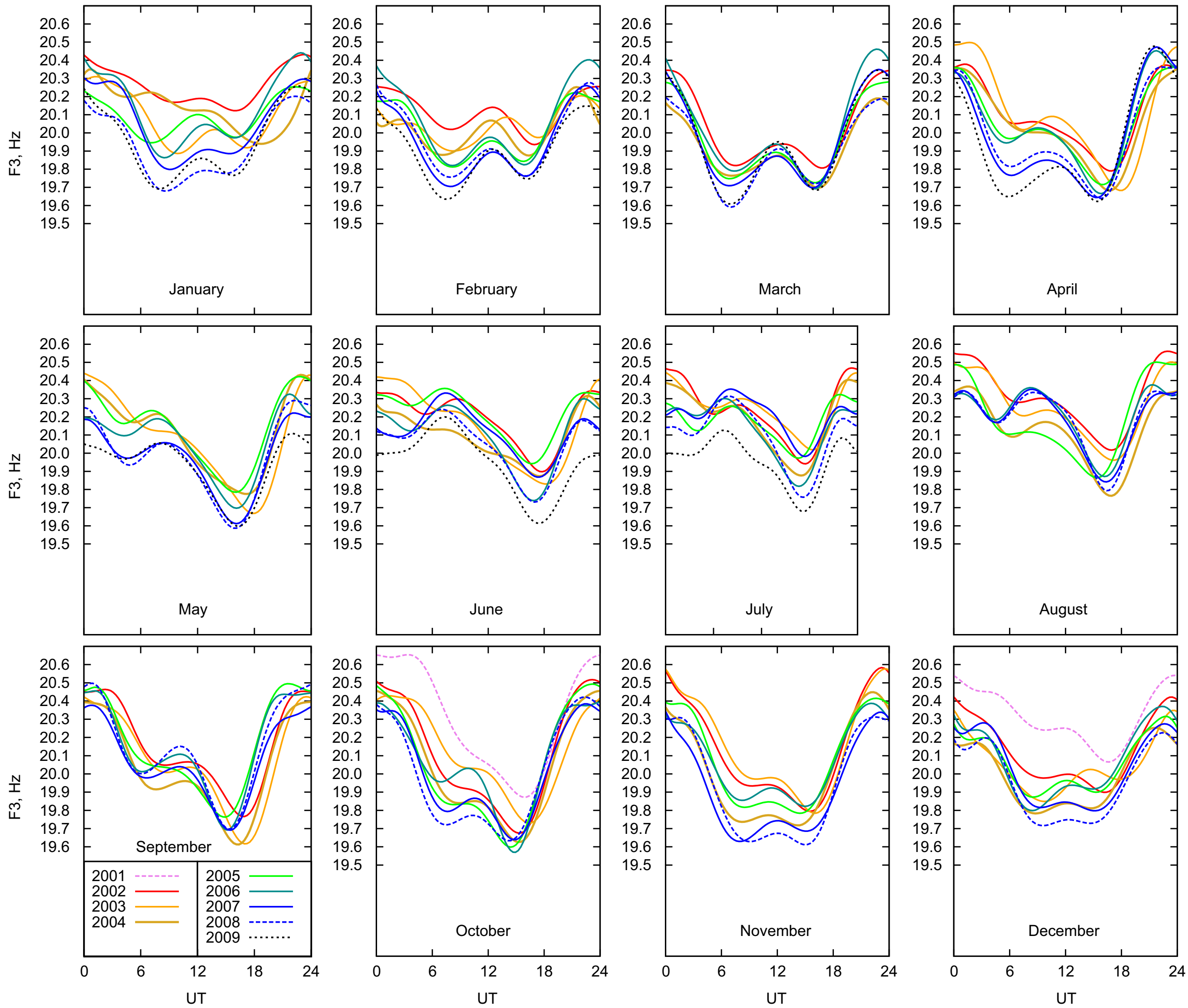

Fig. 3. The same as in Fig. 1 but for the third mode frequency.

16.7°E) for the first and second SR modes are available, e.g. in Nickolaenko et al. (1998).

Thanks to the proximity of Modra Observatory to Nagycenk (103 km), which is very short in comparison to SR wavelength, we decided to use these calibration curves derived for Nagycenk geographical latitude to evaluate the effective lightning areas using our data. The obtained source diameters in degrees are listed in Table 3 and depicted in the middle graph in Fig. 5. As one can see, results from both modes vary similarly. The maxima derived from mode 1 are mostly in the same month as the maxima derived from mode 2. A difference by 21° appears in the estimates deduced from the two modes in a single month. The difference of these values is comparable to the differences in Sátori and Zieger (2003) and Sátori et al. (2007). Due to this variability the effective lightning area is calculated as a mean of the two mode values.

Averages of the effective source widths deduced from the first and the second modes are shown in the lower graph in Fig. 5. This graph and the corresponding values arranged in Table 3 show a pronounced annual variation in the effective lightning areas reaching maxima in spring (April–May) and in autumn (August–September). A mean annual variation calculated as averages of specific months is given in the last but one row of Table 3. The effective source of SR has a minimum width of 39.0° in February and a maximum width of 62.9° in May. Our results, though based on only one solar cycle, verify the annual periodical changes of the effective thunderstorm areas that have been identified by Sátori and Zieger (2003) for the previous solar cycle.

As seen from Table 3, the yearly mean effective source diameter varies in a range from 51.84° in 2005 to 47.97° in 2008. The standard deviation is high, being 8.98 in 2008 up to 12.88 in 2005, as its value is influenced by the inherent annual variation of great amplitude (almost 12°, see the last but one row of Table 3). Though the yearly mean values seem to decrease, no statistically significant trend of yearly mean value of the effective lightning area can be deduced.

Moreover, Sátori and Zieger (2003) and Sátori et al. (2007) showed that the annual changes in source areas, namely the difference between summer solstice (June, July, August) and winter solstice (December, January, February) areas exhibit decadal modulation. They showed that the magnitude of the annual variation slightly but evidently decreased with the decrease in solar activity. However, our data from 2002 to 2009 show that the north–south hemisphere asymmetry in lightning areas, which was significant in the solar cycle maximum, not only decreased, but almost vanished in the deep solar cycle minimum in 2008–2009. The thick full curve interconnecting mean values for June–August and the thick dashed curve interconnecting mean December–February values joined in 2008–2009, see the bottom graph in Fig. 5. From this fact it can be concluded that in the solar cycle minimum, thunderstorms in the NH summer cover the same-size

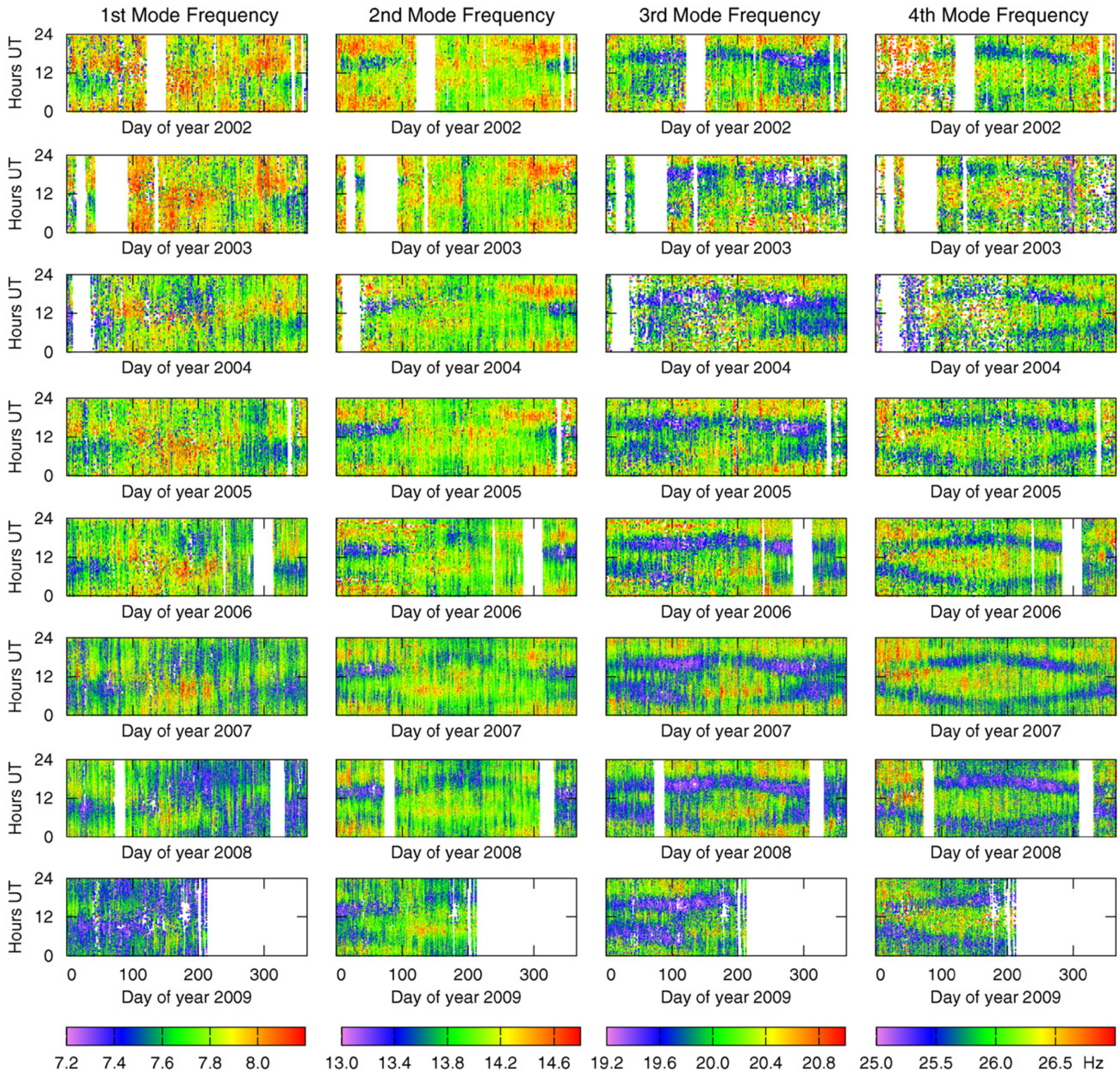

Fig. 4. Diurnal-seasonal frequency variations of the first four modes.

Table 1
The diurnal frequency range (DFR) in mHz deduced from the first Schumann resonance mode (selection of data in MR1 regime).

Year	Jan.	Feb.	Mar.	Apr.	May	Jun.	Jul.	Aug.	Sep.	Oct.	Nov.	Dec.	Mean
2001										200		248	
2002	188	236	212	91	115	200	188	91	152	212	248	261	183
2003	285	315	218	133	115	133	164	145	115	139	267	230	188
2004	273	182	224	158	133	194	182	152	170	182	242	212	192
2005	261	236	164	97	85	188	200	91	152	103	273	242	174
2006	206	212	139	127	133	255	315	194	79	170	236	327	199
2007	212	230	206	133	158	285	273	206	109	145	188	206	196
2008	248	242	200	158	176	285	273	145	109	158	164	182	195
2009	200	139	164	121	176	218	164						
Mean 2002–2008	239	236	195	128	131	220	228	146	127	158	231	237	

area as thunderstorms during the SH summer. This finding is in harmony with a decrease of the effective lightning area deduced from Nagycenk data for NH summer of 1996 (former solar minimum) by Sátori et al. (2007). Naturally, similar observations covering the anomalous minimum of 2008–2009 could not be shown there.

The decrease of the effective lightning region diameters in the NH summer months to the values typical for the SH summer

Table 2
The diurnal frequency range (DFR) in mHz from the 2nd Schumann resonance mode (selection of data in MR1 regime).

Year	Jan.	Feb.	Mar.	Apr.	May	Jun.	Jul.	Aug.	Sep.	Oct.	Nov.	Dec.	Mean
2001										356		577	
2002	481	577	413	212	135	231	144	192	279	385	490	644	349
2003	500	673	442	135	135	173	221	154	288	423	433	519	341
2004	519	606	471	260	135	183	202	135	250	433	548	635	365
2005	606	587	500	192	96	250	240	231	269	288	519	712	374
2006	625	625	596	365	202	298	356	221	192	308	471	673	411
2007	519	615	481	163	260	423	404	231	135	269	500	596	383
2008	577	644	596	202	298	404	481	308	163	231	529	442	406
2009	462	279	423	163	442	375	413						
Mean 2002–2008	547	618	500	218	180	280	293	210	225	334	499	603	

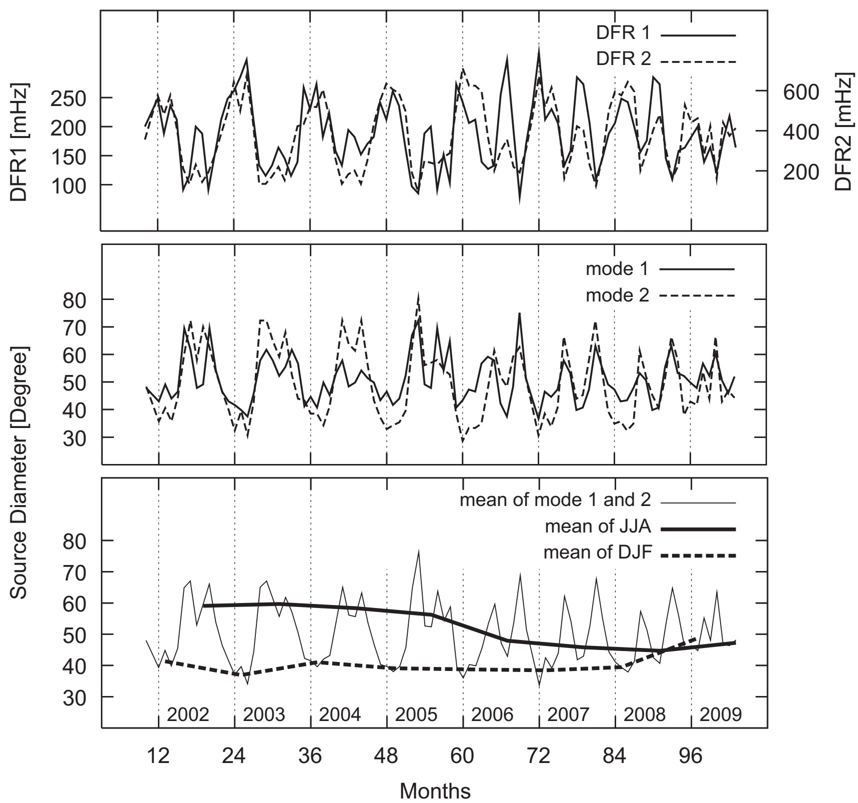

Fig. 5. Variations of the diurnal frequency range – DFR – of the 1st and the 2nd modes (upper graph). Variations of the effective lightning area month by month deduced from DFR of the 1st mode and of the 2nd mode (middle graph). The lower graph shows the mean of the two modes (thin full line). The thick full curve connects NH summer data (mean of June, July and August) and the thick dashed curve connects SH summer data (mean of December, January and February). Both curves merge during the deep solar minimum in 2008–2009.

months (December–February) caused that semi-annual variation dominated in years of the solar cycle minimum, see the bottom graph of Fig. 5.

Though the circular lightning region assumed in the model is centred on the equator, in the NH summer months, this region widens and covers not only the tropics but also middle latitudes. As mentioned above, the lightning region diameters presented here are likely underestimated. If we changed the method of frequency determination for complex demodulation the obtained diameters might be even larger (compare the diameters given in Sátori et al., 2007) and the effective lightning region might expand up to higher middle latitudes.

One of the mechanisms to explain the above discussed reduced size of the effective thunderstorm area in NH leaving SH unchanged was suggested in Sátori et al. (2007) and is as follows. In the NH summer, a lot of lightning activity occurs also at higher-middle latitudes. It has been shown that lightning over Britain and Germany follows the solar activity (Stringfellow, 1974; Schlegel et al., 2001). As there is no corresponding lightning belt in higher middle latitudes in the SH, the reduced solar activity would affect only NH lightning. The Optical Transient Detector satellite lightning observations over North Europe ($>50°$N) also showed a minimum in flash rate in the solar cycle minimum of 1996–1997, see also Sátori et al. (2007). Unfortunately, there are no similar high-latitudinal flash observations covering the anomalous minimum of 2008–2009.

Finally, Fig. 6 depicts the results of spectral analyses of the DFR temporal variations for the first two SR modes. Both modes show maxima around the annual and semi-annual periods and higher annual harmonics appear as well. It is interesting that despite our data were taken about 10 years later and from longer interval (92 months), we obtain the same result as Nickolaenko et al. (1998), namely that the amplitude of the semi-annual period is larger than that of the annual period in case of the first SR mode. The

Table 3
Source diameter in degrees deduced from DFR for the 1st and 2nd SR modes. Standard deviations are also given.

Year	Mode	Jan.	Feb.	Mar.	Apr.	May	Jun.	Jul.	Aug.	Sep.	Oct.	Nov.	Dec.	Yearly mean	Std. (σ)
2001	1										47.8		43.0		
	2										48.3		35.7		
2002	1	49.1	44.0	46.5	69.5	61.7	47.8	49.1	69.5	54.2	46.5	43.0	41.7		
	2	40.6	35.7	44.5	60.2	72.3	58.0	70.0	62.6	53.7	46.6	40.0	32.4	51.63	11.21
2003	1	39.8	37.5	45.9	57.8	61.7	57.8	52.2	55.5	61.7	56.7	41.2	44.6		
	2	39.5	30.7	42.9	72.3	72.3	65.0	59.2	68.0	52.7	43.9	43.3	38.5	51.70	11.50
2004	1	40.7	49.8	45.2	53.2	57.8	48.4	49.8	54.2	51.4	49.8	43.4	46.5		
	2	38.5	34.3	41.2	55.2	72.3	63.8	61.4	72.3	56.1	43.3	37.1	32.9	49.94	10.40
2005	1	41.7	44.0	52.2	67.0	72.4	49.1	47.8	69.5	54.2	64.8	40.7	43.4		
	2	34.3	35.4	39.5	62.6	80.2	56.1	57.0	58.0	54.5	52.7	38.5	28.6	51.84	12.88
2006	1	47.3	46.5	56.7	59.2	57.8	42.2	37.5	48.4	75.1	51.4	44.0	36.7		
	2	33.3	33.3	34.9	47.7	61.4	52.0	48.3	59.2	62.6	51.4	41.2	30.7	48.28	10.85
2007	1	46.5	44.6	47.3	57.8	53.2	39.8	40.7	47.3	63.1	55.5	49.1	47.3		
	2	38.5	33.8	40.6	66.5	55.2	43.9	45.2	58.0	72.3	54.5	39.5	34.9	48.96	9.71
2008	1	43.0	43.4	47.8	53.2	50.6	39.8	40.7	55.5	63.1	53.2	52.2	49.8		
	2	35.7	32.4	34.9	61.4	52.0	45.2	40.6	51.4	66.4	58.0	38.0	42.9	47.97	8.98
2009	1	47.8	56.7	52.2	60.4	50.6	45.9	52.0							
	2	41.7	53.7	43.9	66.5	42.9	46.8	44.3							
Mean 2002–2008	1 & 2	40.6	39.0	44.3	60.3	62.9	50.6	50.0	59.2	60.1	52.0	42.2	39.4		
Std. (σ)	1 & 2	4.5	5.9	5.8	6.6	9.0	8.1	8.9	7.8	7.2	5.7	4.0	6.5		

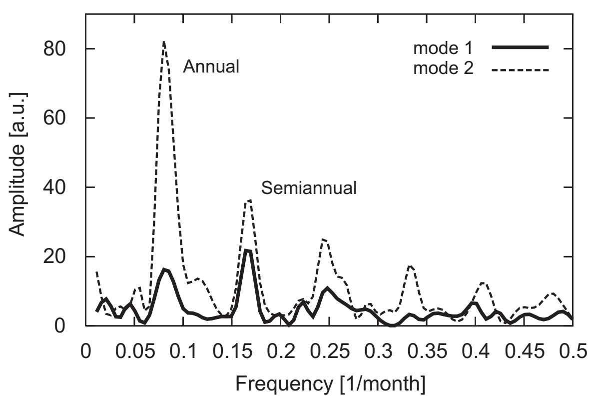

Fig. 6. Amplitude spectra of DFR for the first and second SR modes. Data from 92 months were used.

semi-annual variation can be attributed to the periodical lightning activity at equinoxes while the north–south asymmetry in the land distribution over the globe can explain the one-year period.

5. 11-Year variation of the SR parameters

As the source–observer geometry repeats every year it is understandable that the diurnal frequency variation curves for all years and for all 4 investigated modes have nearly the same pattern.

The inter-annual difference between the curves seen in Fig. 1 exhibits a systematic or quasi-systematic decrease of frequency from 2001–2002 (year of the solar cycle maximum) to 2008–2009 (year of the solar cycle minimum). The full bold curve is for 2001, and the lowest thin dotted curve is for 2009. The average difference between the curve for 2002 and the curve for 2008 is 0.2–0.4 Hz. Similar quasi-systematic decrease of the diurnal variation curves is evident in Figs. 2 and 3.

To study the long-term changes the monthly mean values of the first, second, third and fourth mode frequencies and Q-factors were calculated and the obtained values are depicted in Fig. 7. The third mode manifests the most pronounced annual variation but a decrease of all frequencies and all Q-factors toward the solar cycle minimum in 2009 is evident. GOES satellite 5 min averages of the

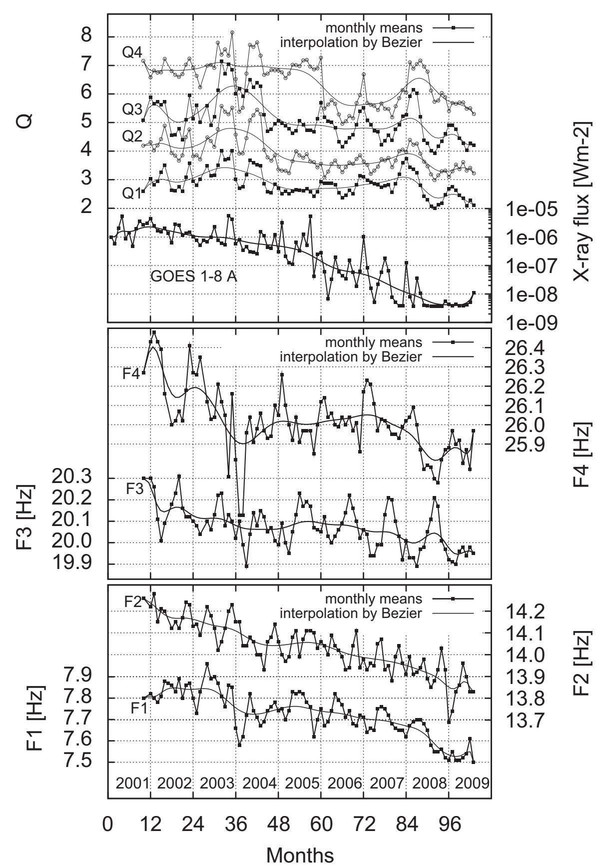

Fig. 7. Monthly mean values of the first four Schumann resonance frequencies and the X-ray flux. Smooth full lines are the Bezier interpolations. Monthly means of Q-factors are also depicted. The yearly mean of the first mode frequency for June 2002–May 2003 is 7.84 Hz; the yearly mean for June 2008–May 2009 is 7.55 Hz. All SR frequencies and all Q-factors exhibit pronounced decrease toward the solar cycle minimum.

solar X-radiation flux in 0.1–0.8 nm range (http://goes.ngdc.noaa.gov/data/avg/) were used to compute monthly means and the results are plotted in Fig. 7 too. A smooth full line is the Bezier interpolation. A deep minimum of this flux appeared from June 2008 up to May 2009. That is why all yearly means are calculated

Table 4
Mean frequencies and Q-factors of the first 4 SR modes in different phases of the studied solar cycle. Frequencies drop for every SR mode due to the global changes in the ionosphere and they follow the decrease in the solar X-ray flux.

	F1	Q1	F2	Q2	F3	Q3	F4	Q4	X-ray 1–8 A
Solar maximum (June 2002–May 2003)	7.84	2.99	14.16	4.10	20.12	5.12	26.16	6.80	1.23×10^{-6}
Mean for Jan 2007–Dec 2007	7.68	2.99	13.97	3.65	20.04	4.76	26.03	5.65	4.78×10^{-8}
Solar minimum (June 2008–May 2009)	7.55	2.34	13.87	3.30	20.01	4.39	25.84	5.83	4.05×10^{-9}

from June to May of the next year. The yearly mean value of the X-ray flux in the wavelength interval 0.1–0.8 nm decreased from 1.23×10^{-6} W m^{-2} (June 2002–May 2003) to 4.05×10^{-9} W m^{-2} (June 2008–May 2009). In the same period, e.g. the first mode frequency dropped from 7.84 Hz (June 2002–May 2003) to 7.55 Hz (June 2008–May 2009).

The yearly mean values of frequencies and Q-factors of the studied SR modes in the solar maximum are arranged in the first row in Table 4, the corresponding values for the solar minimum in the last row. For comparison, the yearly mean values for 2007 when the X-ray flux reached the level of the previous solar cycle minimum are listed in the second row.

A decrease of mode frequencies and quality factors over the solar cycle has been explained by Sátori et al. (2005) from the point of view of changes in the two characteristic layers, which represent the upper boundary of the waveguide, and which are responsible for ELF wave propagation (see also Greifinger et al., 2007). On the 11-year time scale, the solar output in the X-ray range varies on average by 2 orders of magnitude, in the ultraviolet range by a factor of 2 and both are proportional to the solar activity, measured by sunspot numbers. Cosmic rays, which are another ionization source affecting mainly the lower characteristic layer (50–60 km), also vary with the solar cycle but inversely. According to Sátori et al. (2005) changes of the X-ray radiation dominate the variations in the conductivity profile within the upper characteristic layer (the 90–100 km portion of the E-region). The decrease of this conductivity by up to one order of magnitude over the solar cycle is responsible for the observed SR frequencies decrease by several tenths of Hz. Furthermore, the change in the scale height of the conductivity profile modulates the reflection/dissipation effects within the upper characteristic layer and, therefore, the Q-factors of the resonator.

Our observations support the findings of Sátori et al. (2005) that the variations of SR frequencies are in phase with the solar X-ray output over the solar cycle, i.e. over the 11-year time scale, and our result at another station serves to verify their global behaviour. Our electric field component data show that the frequency of the first mode decreased by 0.29 Hz from the latest solar maximum to the minimum in 2008–2009. The value obtained here is much greater than the corresponding value of 0.07 Hz deduced by Sátori et al. (2005) but for the previous solar cycle. Similarly, a decrease by 0.29 Hz was obtained here for the second mode frequency while 0.10 Hz was determined by Sátori et al. (2005). The greater drop of these frequencies in the 2008–2009 solar cycle minimum can be attributed to the very low level of solar activity and thus also a very low level of solar output in the X-ray range since June 2008, which is by one order of magnitude lower than that during the previous minimum of 1996–1997.

The level of the solar X-ray radiation (in 0.1–0.8 nm range) in the previous solar minimum was about 3.6×10^{-8} W m^{-2} (Sátori et al., 2005). In the studied solar cycle, the X-ray flux of this order was reached in 2007 (January–December). In 2007, according to our observations, the yearly mean value of the first Schumann resonance frequency was 7.68 Hz. It means that by that time the first SR mode decreased by 0.16 Hz, a value similar to the values obtained by Sátori et al. (2005) from the SR magnetic component data. A decrease of the other modes by 0.19, 0.08 and 0.13 Hz, respectively, reached in 2007 is also comparable with the results obtained for the previous solar minimum.

Unfortunately, no Q-factor values were evaluated from Nagycenk electric component data. Decreases by 0.65, 0.80, 0.73 and 0.97 of the Q-factor for the four studied SR modes were found here (Table 4). As expected, these values are greater than the decreases reported in Sátori et al. (2005) for the previous solar cycle though deduced from the SR magnetic component.

6. Conclusions

Observations of SR at Modra that cover the period from the solar cycle maximum in 2001–2002 to the anomalous solar cycle minimum in 2008–2009 are in harmony with the results of Sátori et al. (2005) but our measurements reveal greater decrease of the first two SR mode frequencies.

The decrease of the Q-factors derived here from the electric component is found greater than in the previous minimum of solar activity derived from the magnetic component.

It was found that the effective lightning area in the NH summer months (June, July, August) decreased so much that the difference between the NH summer and the SH summer areas not only diminished with the decrease in solar activity, but even almost vanished during the deep minimum of 2008–2009. At the same time, no statistically significant decrease of the yearly mean diameter of the effective lightning area was found.

As discussed in Section 4, the higher middle latitude lightning region in the NH likely shrank or almost vanished with the decrease in solar activity. In other words it seems that much less lightning occurred in the northern higher latitudes in summer in the years of the deep solar cycle minimum of 2008–2009 than in other phases of the solar cycle. Though this finding is supported by the two studies of local lightning flash rate it should be verified in further investigations using data from worldwide lightning networks. It should be noted that a lot of lightning still occurred in the tropics.

This effect of diminishing of the effective lightning area in NH summer months can be identified also in results of Sátori and Zieger (2003) and Sátori et al. (2007) for the previous "ordinary" solar cycle minimum but it is not as pronounced as here using the data from the anomalously deep minimum.

Acknowledgements

This work was supported by the grant 1/0521/08 of the Scientific Grant Agency VEGA. Authors are thankful to National Oceanic and Atmospheric Administration (NOAA) for the X-ray data from GOES-10.

References

Balser, M., Wagner, C.A., 1960. Observation of Earth-ionosphere cavity resonances. Nature 188, 638–641.
Bliokh, P.V., Nickolaenko, A.P., Filippov, Yu.F., 1980. Schumann resonances in the Earth-ionosphere cavity. In: D.Ll. Jones, (Ed.), Peter Peregrinus, London.
Füllekrug, M., Fraser-Smith, A.C., Schlegel, K., 2002. Global ionospheric D-layer height monitoring. Europhys. Lett. 59, 626–629.

Greifinger, P.S., Mushtak, B.C., Williams, E.R., 2007. On modeling the lower characteristic ELF altitude from aeronomical data. Radio Sci. 42 (2), RS2S12.

Kostecký, P., Ondrášková, A., Rosenberg, L., Turňa, L'., 2000. Experimental setup for the monitoring of Schumann resonance electric and magnetic field variations at the Geophysical Observatory at Modra-Piesok. Acta Astron. et Geophys. XXI–XXII, 71–92.

Kulak, A., Kubisz, J., Michalec, A., Ziba, S., Nieckarz, Z., 2003. Solar variations in extremely low frequency propagation parameters: 2. Observations of Schumann resonances and computation of the ELF attenuation parameter. J. Geophys. Res. 108 (A7), 1271.

Nickolaenko, A.P., 1997. Modern aspects of Schumann resonance studies. J. Atmos. Sol.–Terr. Phys. 59 (7), 805–816.

Nickolaenko, A.P., Hayakawa, M., 2002. Resonances in the Earth-Ionosphere Cavity. Kluwer Academic Publishers, Dordrecht/Boston/London, 380pp.

Nickolaenko, A.P., Rabinowicz, L.M., 1995. Study of the annual changes of global lightning distribution and frequency variations of the first Schumann resonance mode. J. Atmos. Sol.–Terr. Phys. 57, 1345–1348.

Nickolaenko, A.P., Sátori, G., Zieger, V., Rabinowicz, L.M., Kudintseva, 1998. Parameters of the global thunderstorm activity deduced from the long-term Schumann resonance records. J. Atmos. Sol.–Terr. Phys. 60, 387–399.

Ogawa, T., Tanaka, Y., Yasuhara, M., 1969. Schumann resonances and world-wide thunderstorm activity. Diurnal variations of the resonant power of natural noise in the Earth-ionosphere cavity. J. Geomagn. Geoelec. 21, 447–452.

Ondrášková, A., Kostecký, P., Ševčík, S., Rosenberg, L., 2007. Long-term observations of Schumann resonances at Modra Observatory. Radio Sci. 42, RS2S09. doi: 10.1029/2006RS003478.

Price, C., Melnikov, A., 2004. Diurnal, seasonal and inter - annual variations in the Schumann resonance parameters. J. Atmos. Sol.-Terr. Phys. 66, 1179–1185.

Sátori, G., 1996. Monitoring Schumann resonances II. Daily and seasonal frequency variations. J. Atmos. Terr. Phys. 58, 1483–1488.

Sátori, G., Lemperger, I., Bór, J., 2007. Modulation of annual and semiannual areal variations of global lightning on the 11-year solar cycle. In: Second International Symposium on Lightning Physics and Effects, Vienna, April 19 and 20, 2007.

Sátori, G., Mushtak, V., Williams, E.R., 2009. Schumann resonance signatures of global lightning activity. In: Betz, H.D., Schumann, U., Laroche, P. (Eds.), Lightning: Principles, Instruments and Applications. Springer, pp. 641.

Sátori, G., Williams, E., Boccippio, D.J., 2003. On the dynamics of the north–south seasonal migration of global lightning. AGU, Fall Meeting 2003, abstract \#AE32A-0167.

Sátori, G., Williams, E., Boldi, R., Füllekrug, M., 2000. Systematic variations of Schumann resonance frequencies on the 11-year solar cycle at multiple stations. EOS Trans. AGU 81 (48), A12B–01.

Sátori, G., Williams, E., Mushtak, V., 2005. Response of the Earth-ionosphere cavity resonator to the 11-year solar cycle in X-radiation. J. Atmos. Sol.–Terr. Phys. 67, 553–562.

Sátori, G., Zieger, B., 1996. Spectral characteristics of Schumann resonances observed in Central Europe. J. Geophys. Res. 101, 29663–29669.

Sátori, G., Zieger, B., 2003. Areal variations of the worldwide thunderstorm activity on different time scales as shown by Schumann resonances. In: Proceeding of the 12th ICAE, Versailles, France, Global Lightning and Climate, pp. 1–4.

Schlegel, K., Diendorfer, G., Thern, S., Schmidt, M., 2001. Thunderstorms, lightning and solar activity—Middle Europe. J. Atmos. Sol.–Terr. Phys. 63 (16), 1705–1713.

Schumann, W.O., 1952. On the free oscillations of a conducting sphere which is surrounded by an air layer and a ionosphere shell. Zs. Naturforschung 7a, 149–154 in German.

Stringfellow, M.F., 1974. Lightning incidence in Britain and the solar cycle. Nature 249, 332–333.

Williams, E.R., 1992. The Schumann resonance: a global tropical thermometer. Science 256, 1184–1187.